BIOCHEMISTRY
Including biophysical chemistry & molecular biology
Article

Biochemistry **2009**, *48*, 8387–8395 8387
DOI: 10.1021/bi9008402

Engineering the Substrate Binding Site of Benzoylformate Decarboxylase†

Alejandra Yep‡ and Michael J. McLeish*,‡,§

‡*College of Pharmacy, University of Michigan, Ann Arbor, Michigan 48109, and* §*Department of Chemistry and Chemical Biology, IUPUI, Indianapolis, Indiana 46202*

Received May 18, 2009; Revised Manuscript Received July 20, 2009

ABSTRACT: Benzoylformate decarboxylase (BFDC) and pyruvate decarboxylase (PDC) are both thiamin diphosphate-dependent enzymes. The two share a common three-dimensional structure and catalyze a similar chemical reaction, i.e., decarboxylation of 2-keto acids. However, they vary significantly in their substrate utilization pattern. In particular, BFDC has extremely limited activity with pyruvate, while PDC has no activity with benzoylformate. Here we report our progress, using a semirandom approach, toward converting BFDC into an efficient pyruvate decarboxylase. From the structure of BFDC in complex with *R*-mandelate, 12 residues within a 5 Å radius from the inhibitor molecule were selected and subjected individually to site-saturation mutagenesis. Each variant was screened for its ability to decarboxylate five different substrates, i.e., benzoylformate, 2-ketohexanoate, 2-ketopentanoate, 2-ketobutanoate, and pyruvate. The first round of mutagenesis showed that changes in Thr377 and Ala460 resulted in an altered substrate spectrum which included higher activity toward pyruvate. Two variants, T377L and A460Y, were selected as the starting point of a second round of site-saturation mutagenesis. In both cases, the T377L-A460Y double mutant proved to be the only new variant with significantly improved catalytic activity toward pyruvate. When compared to the wild-type enzyme, based on k_{cat}/K_m values, the T377L-A460Y variant showed an 11000-fold improvement in the ratio between pyruvate and benzoylformate utilization. This double mutant displays a K_m value for pyruvate of 2 mM as well as a k_{cat}/K_m value for pyruvate which is only 70-fold lower than that of *Zymomonas mobilis* PDC.

The ability to modify the substrate specificity of enzymes with the ultimate aim of designing tailor-made products is an elusive goal of protein science. Directed evolution strategies include both random and targeted mutagenesis (*1*). In the presence of structural data, rational approaches are generally favored, site-directed mutagenesis being both relatively easy and inexpensive, and in some cases, this targeted approach has been successful (*2*, *3*). In the absence of structural information, random methods have been applied also with varying degrees of success (*4*, *5*). In these cases, the availability of a selection method is practically a requirement due to the large number of variants generated.

Benzoylformate decarboxylase (BFDC[1], EC 4.1.1.7) from *Pseudomonas putida* (*Pp*BFDC) is a thiamin diphosphate (ThDP)-dependent decarboxylase that catalyzes the formation of benzaldehyde and carbon dioxide from benzoylformate (Scheme 1). It is part of a pathway that allows bacteria to grow using (*R*)-mandelate as the sole carbon source (*6*). *Pp*BFDC has been kinetically characterized by steady-state and stopped-flow methods combined with site-directed mutagenesis (*7*, *8*). Its crystal structure has also been solved, both alone and in complex with inhibitors and covalently bound intermediates (*7*, *9*, *10*). Pyruvate decarboxylase (PDC, EC 4.1.1.1) from *Zymomonas mobilis* (*Zm*PDC) catalyzes the conversion of pyruvate to acetaldehyde and carbon dioxide (Scheme 1). It belongs to the same family as BFDC and shares with it a common protein fold and chemical mechanism (*11*). Their substrate preferences, however, differ widely, and with the exception of the residues involved in the binding of ThDP, there is no sequence conservation in the active site (*12*). In particular, BFDC lacks the two contiguous histidine residues that are conserved among most ThDP-dependent decarboxylases, including the various PDCs, as well as indolepyruvate decarboxylase (IPDC), phenylpyruvate decarboxylase (PPDC), and the branched chain 2-keto acid decarboxylase, KdcA. In BFDC, these two histidine residues are replaced by two leucines. However, two histidines from different loops come together to occupy similar spatial positions and, it was presumed, to perform roles similar to those of PDC (*9*).

As part of our ongoing efforts to evolve the mandelamide/mandelate pathway (*6*, *13*) into a novel lactamide pathway (*12*, *14*), we are interested in determining the rules that govern substrate specificity in ThDP-dependent decarboxylases. More specifically, we want to convert BFDC into a PDC, which would involve shifting the substrate preference from binding a phenyl group to binding a methyl group.

Previously, we have shown that BFDC has very limited activity with pyruvate, and PDC has no activity with benzoylformate (*12*). Initial attempts to exchange specificity in this family of enzymes provided mixed results. Site-directed mutations based on structural data were able to improve decarboxylation of alternative substrates in *Zm*PDC (*12*), but attempts to use the same approach to improve pyruvate usage in *Pp*BFDC (*12*) and KdcA (*15*) were not particularly successful. Random methodologies such as directed evolution using error-prone PCR and gene

†This work was supported by NSF Frontiers in Integrative Biology Grant (EF-0425719).

*To whom correspondence should be addressed. Phone: (317) 274-6889. Fax: (317) 274-4701. E-mail: mcleish@iupui.edu.

[1]Abbreviations: BFDC, benzoylformate decarboxylase; PDC, pyruvate decarboxylase; ThDP, thiamin diphosphate; BF, benzoylformate; 2KH, 2-ketohexanoate; 2KP, 2-ketopentanoate; 2KB, 2-ketobutyrate; Pyr, pyruvate; HLADH, horse liver alcohol dehydrogenase; YADH, yeast alcohol dehydrogenase; wt, wild-type.

Scheme 1: Reaction Catalyzed by Benzoyformate Decarboxylase (BFDC) and Pyruvate Decarboxylase (PDC)

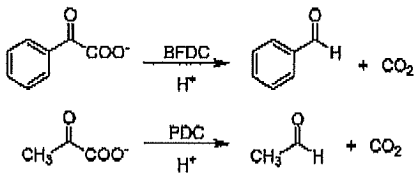

shuffling are common alternatives to rational approaches in enzyme engineering (*4*). Semirandom methodologies have also been employed to change substrate specificity. In those instances, rational design and directed evolution were integrated by performing saturation mutagenesis on active site residues identified through X-ray crystallography (*16*, *17*) or even molecular modeling (*18*, *19*). Unfortunately, the large number of variants generated in these approaches and the low percentage of variants that are potentially useful, makes a selection method almost a necessity. Although less efficient than selection, a high throughput approach can also be used to screen large numbers of variant enzymes. Recently, we developed a microplate assay for BFDC activity that permitted identification in crude cell extracts of BFDC variants with k_{cat} values ranging over 3 orders of magnitude (*20*). In this work, we have applied a semirandom methodology to alter the substrate specificity of *Pp*BFDC toward small aliphatic 2-keto acids. A subset of BFDC residues was rationally chosen on the basis of X-ray structures and subjected to site-saturation mutagenesis. The microplate assay was extended to test activity in whole cell extracts with several 2-keto acid substrates. Overall, this approach allowed us to generate *Pp*BFDC variants with improved binding and catalytic activity toward pyruvate. Given that the assay can be used with a variety of substrates, it has the potential to be used to examine changes in substrate specificity in any member of this family of enzymes.

MATERIALS AND METHODS

Materials. Oligonucleotides were synthesized by IDT Technologies. NADH, HLADH, YADH, and 2-keto acids were purchased from Sigma (St. Louis, MO). *Dpn*I was from New England Biolabs, and *Pfu* polymerase was from Stratagene. DNA sequencing was carried out at the University of Michigan DNA sequencing core.

Generation of a Strain for Screening of Pyruvate Decarboxylase Activity. The *E. coli* strain FMJ39, which lacks lactate dehydrogenase activity (*21*), was purchased from the *E. coli* Genetic Resource Center at Yale University. Strain FMJ39(DE3) was generated using a lysogenesis kit purchased from Invitrogen. Both strains were grown at 37 °C in LB media supplemented with 30 μg/mL streptomycin and stored at −80 °C with 16% v/v glycerol.

Site-Saturation Mutagenesis. Site-saturation mutagenesis was carried out with the QuikChange methodology and degenerate primers using pETBFDC-His as the parental plasmid as previously described (*20*). For double mutants, the plasmid containing the appropriate single mutation was used. The purified mixture of plasmids was transformed into electrocompetent MegaX DH10B T1 cells (Invitrogen) using an Eppendorf 2510 micropulser, and plated on LB agar supplemented with 50 μg/mL kanamycin and 30 μg/mL streptomycin. Colonies grown overnight were collected, resuspended in saline solution, and subjected to plasmid DNA extraction. This mixed population of mutant plasmids was used for transformation of chemically competent *E. coli* FMJ39(DE3) cells. Individual colonies obtained in this manner were randomly selected and inoculated in 0.9 mL cultures of overnight express TB self-inducing media (Novagen) in deep-well 96-well plates (Abgene). The inoculates were covered with a gas permeable membrane (Abgene) and grown for 16−20 h at 37 °C with 300 rpm agitation. Samples from the cultures were mixed with glycerol (final concentration 16% v/v) and stored at −80 °C. The remainder of the FMJ39(DE3) cultures were lysed with the commercial reagent FastBreak (Novagen), in the presence of 0.1 units/mL DNase I and lysozyme, and incubated for 30 min at room temperature with 300 rpm shaking. These whole cell lysates were utilized as the enzyme source for screening of activity. Each plate consisted of cultures from 88 randomly selected colonies and 8 controls.

Screening for Enzyme Activity. The screening assay is an adaptation to the microplate reader format from the coupled assay for 2-keto acid decarboxylase activity (*22*). The mixture contained 0.28 mM NADH, 1 unit/mL of the appropriate alcohol dehydrogenase, 1 mM $MgSO_4$, 0.5 mM ThDP, and the requisite 2-keto acid in 100 mM potassium phosphate buffer (pH 6.0), in a final volume of 200 μL. The activity of each plate of randomly selected colonies was assayed with five substrates: 1 mM benzoylformate (BF), 10 mM 2-ketohexanoate (2KH), 10 mM 2-ketopentanoate (2KP), 10 mM 2-ketobutyrate (2KB), and 10 mM pyruvate (Pyr). The reaction mixture was placed in an UV transparent 96-well microplate and allowed to equilibrate at 30 °C in a Biotek ELx808 IU plate reader. A background run of 1 min at 340 nm was recorded. The reaction was then started with the addition of 20 μL of the lysates, and the decrease in absorbance at 340 nm was recorded for an additional minute. Controls included TB overnight express and FMJ39(DE3) cells harboring each of the expression vectors pET24a, pETBFDC-His, pETBFDCA460I, and pETBFDCF464I. The last two were available from a previous study (*12*).

Enzyme Purification and Kinetic Characterization. After analysis of activity data, selected glycerol stocks were grown in 5 mL cultures. Their plasmid DNA was extracted and sequenced to identify the codon in the randomized position. The BFDC gene in the colonies selected for protein expression and purification was sequenced in its entirety to ensure that the only mutation was in the desired codon. Following transformation into BL21(DE3)pLysS cells, protein expression and purification was conducted as previously described (*15*). Homogeneous fractions were pooled, concentrated, and their buffer exchanged for BFDC storage buffer (100 mM potassium phosphate at pH 6.0, 0.5 mM ThDP, 1 mM $MgSO_4$, and 10% glycerol) before being kept at −80 °C.

The activity assays with the purified enzymes have been described elsewhere (*22*). The assay contained the appropriate substrate, NADH, and HLADH (YADH was used when pyruvate or 2-ketobutyrate were substrates) in 100 mM potassium phosphate buffer (pH 6.0) with a final volume of 1 mL. The reaction was carried out at 30 °C and was initiated by the addition of the BFDC variant. Kinetic data were fit to the Michaelis−Menten equation using SigmaPlot 9.0.1. Radar plots were prepared using Excel 2007 (Microsoft).

Sequence Analysis and Figures. Sequence analysis was initially performed using ClustalW and manually refined incorporating structural information in BioEdit. Figures were generated using Swiss-PdbViewer (*23*) and Pov-Ray (www.povray.org).

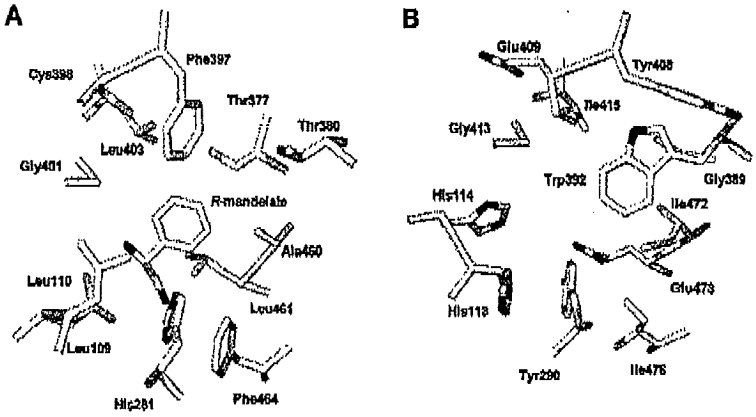

FIGURE 1: (A) Residues in the substrate binding site of BFDC identified as candidates for saturation mutagenesis. (B) Structural equivalents of these residues in *Zm*PDC. Although ThDP has been omitted for clarity, the positions of the cofactors are superimposable in the two active sites. The figure was prepared with Swiss-PdbViewer (http://www.expasy.org/spdbv/) using coordinates from PDB 1MCZ (BFDC) and 1ZPD (*Zm*PDC).

Table 1: Partial Alignment of PDCs and BFDCs[a]

	Organism[b]	Locus									
BFDCs	Pse_pu	AAC15502	107	EALLT	278	FRYHQY	375	ESTSTTA	397	FCA-AGGLG	458 YGALRWFA
	Pse_st	ABN80423	107	EALLT	278	FRYHQY	375	ESTSTTA	397	FCA-AGGLG	458 YGALRWFA
	Pse_ae	AAG08286	121	EAMLA	278	FRYHQF	375	ESTSIVT	397	FPA-AGGLG	458 YGALRWFA
	Bra_ja	BAC51681	121	DPFLA	288	FSYHVE	384	EAPGARS	406	TMD-SGGLG	467 YAALQDFA
	Bur_ma	EDP87859	121	EPFLA	288	FTYHIE	387	EAPSARP	409	TMD-SGGLG	470 YAALQDFA
	Str_co	CAB76356	107	EANLA	277	FRYHEH	374	ESTSINA	396	FPA-AGGLG	457 YGALRWFG
PDCs	Zym_mo	AAV89984	111	VLHHA	287	FNDYST	387	EIGDSWF	408	YEMQWGHIG	470 YTIEVMIH
	Ace_pa	AAM21208	111	ILHHT	287	FNDYST	383	EIGDSWF	403	LEMQWGHIG	465 YVIEIAIH
	Zym_pa	AAM49566	110	ILHHT	286	FNDYAT	382	EIGDSWF	403	LEMQWGHIG	464 YVIEIAIH
	Mic_ae	BAG03497	111	LVHHS	285	FYDTIT	379	EIGTSYS	399	GQGSWMSIG	462 YTIERLIH
	Sar_ve	AAL18557	111	LLHHT	282	MSDMNL	377	DIGDAYY	402	GWAFYLSIG	464 YTIERVIQ
	Sta_au	CAI79816	111	YVHHS	282	LIDSAT	377	DQGTSFF	398	GQPLWGSIG	460 YTVERLIH
	Myc_av	AAS03100	120	ALHHS	293	FTDMVS	391	DQGTSFY	412	GQPLWGSIG	474 YTVERAIH

[a] The *Pp*BFDC residues mutated in this study, and their counterparts in other BFDCs and PDCs, are in boldface. [b] Pse_pu, *Pseudomonas putida*; Pse_st, *Pseudomonas stutzeri*; Pse_ae, *Pseudomonas aeruginosa*; Bra_ja, *Bradyrhizobium japonicum*; Bur_ma, *Burkholderia mallei*; Str_co, *Streptomyces coelicolor*; Zym_mo, *Zymomonas mobilis*; Ace_pa, *Acetobacter pasteurianus*; Zym_pa, *Zymobacter palmae*; Mic_ae, *Microcystis aeruginosa*; Sar_ve, *Sarcina ventriculi*; Sta_au, *Staphylococcus aureus*; Myc_av, *Mycobacterium avium*.

RESULTS

Selection of Residues for Mutagenesis. Using the structure of BFDC bound to (*R*)-mandelate, a substrate analogue inhibitor (PDB code 1MCZ (*7*)), as a guide, we found 15 residues to be located within 5 Å of the inhibitor. These included Ser26 and His70, which had been examined previously using saturation mutagenesis (*20*), while preliminary attempts at mutation of Gly25, a conserved residue, had resulted in inactive protein (Yep, A., unpublished observations). For these reasons, the last three residues were not studied in this work. The remaining 12 residues (Figure 1) were found to have a structural counterpart in *Zm*PDC (PDB code 1ZPD (*24*)) and were considered to be viable candidates for mutagenesis.

To expand the analysis, bacterial PDCs and BFDCs available in databases were aligned separately using ClustalW. The two alignments were combined using the information from the

Table 2: Sequences of Primers Used in Saturation Mutagenesis[a]

primer	sequence
L109X	5′-GCGATGATTGGCGTTGAAGTCNNNCTGACCAACGTCGATGCC-3′
L110X	5′-GCGATGATTGGCGTTGAAGCTTTANNNACCAACGTCGATGCCGCC-3′
H281X	5′-GGCGCTCCAGTGTTCCGTTACNNNCAATACGACCCAGTC-3′
T377X	5′-GCGATTTACCTGAACGAGTCGNNNTCAACGACCGCCCAAATGTGG-3′
T380X	5′-CGAGTCGACTTCAACGNNNGCCCAAATGTGGCAGCGC-3′
F397X	5′-CCCTGGTAGCTACTACNNNTGTGCAGCTGGCGGACTG-3′
C398X	5′-CCCTGGTAGCTACTACTTCNNNGCAGCTGGCGGACTG-3′
G401X	5′-GCTACTACTTCTGTGCAGCTNNNGGACTGGGCTTCGCCCTGCC-3′
L403X	5′-CTGTGCAGCTGGCGGANNNGGCTTCGCCCTGCCTGC-3′
A460X	5′-CAACGGCACCTACGGTNNNTTGCGATGGTTTGCCGGCG-3′
L461X	5′-CAACGGCACCTACGGTGCGNNNCGATGGTTTGCCGGCGTTC-3′
F464X	5′-CGGTGCGTTGCGATGGNNNGCCGGCGTTCTCGAAGC-3′

[a] N refers to an equal mixture of A, T, G, and C.

structural alignment of *Pp*BFDC and *Zm*PDC coordinates. Most of the sequences for these two enzymes available in databases correspond to putative enzymes. The only bacterial enzymes with proven 2-keto acid decarboxylase activity are PDC from *Zymomonas mobilis* (*25*), *Sarcina ventriculi* (*26*), and *Acetobacter pasteurianus* (*27*), and BFDC from *Pseudomonas putida* (*28*), *Pseudomonas aeruginosa* (*29*), and *Pseudomonas stutzeri* (*30*). This constraint clusters most of the enzymes of this class in a narrow subset of bacteria, the proteobacteria. Table 1 shows a representative subset of these sequences. Of the residues studied, seven were conserved among the BFDCs. Only Gly401 is conserved between *Pp*BFDC and *Zm*PDC but, whereas it seems well conserved among BFDCs, it is not in PDC sequences. By contrast, Gly389 is fully conserved in the PDCs, presumably to accommodate a bulky aromatic substituent (Trp in *Zm*PDC) at position 392. Given the lack of consensus and in keeping with the less targeted approach, it was decided that all 12 residues should be subjected to mutagenesis.

Site-Saturation Mutagenesis and Screening. Randomization of the chosen positions was carried out as described in the Materials and Methods section, using QuikChange PCR with degenerate primers. The site-saturation mutagenesis protocol and the library quality were validated in a previous study (*20*). Initially, BL21(DE3) cells were chosen as the expression strain for the screening assay. However, when whole cell extracts of BL21(DE3) cells were assayed in the presence of NADH and Pyr, there was sufficient NADH consumption to cause an extremely elevated background, as measured by the decrease in absorbance at 340 nm in the absence of added enzyme. To overcome this, the strain FMJ39(DE3), which lacks lactate dehydrogenase activity (*21*), was used. With this strain, the background was significantly reduced and was comparable for all substrates utilized.

In the initial round of site-saturation mutagenesis, the 12 libraries corresponding to individual positions were screened in 96-well plates. Details of the primers used in library construction are provided in Table 2. At first, we attempted to assay with only BF and Pyr, but the activity with the latter was too close to the detection limit of the screening assay, and variants with improved activity could easily be overlooked. Our previous report had shown that a single mutation could improve BFDC activity toward branched-chain and long chain aliphatic 2-keto acids (*12*). It was thought that variants with improved activity toward Pyr might also have a better activity toward larger aliphatic 2-keto acids, such as 2KB, 2KP, and 2KH; therefore, these three substrates were also added to the screening.

From the results of the first round, it became clear that the substitutions affected some positions more than others. This is exemplified by Figure 2, which shows plots for the activity of individual colonies for three libraries, i.e., one plate per library with BF as a substrate. It is clear that most substitutions in position 464 do not dramatically alter the activity toward BF, whereas substitution of Gly401 generates enzymes with greatly reduced activity. However, position Ala460 seems to be somewhere in the middle, where some substitutions generate inactive variants but many generate alternatives with varying degrees of activity toward the natural substrate of BFDC.

As a way of simplifying the analysis, the activity data for the five substrates were plotted in radar graphs. Activity data from 8 colonies (one column of wells in a 96-well plate) were plotted in each radar graph, a total of 11 graphs per plate. For easy comparison, the activity data from the control wild-type (wt) colony from that plate were included in each plot. Figure 3 shows a typical radar plot in which most colonies keep the same substrate usage pattern as that containing the wt BFDC, albeit with different levels of activity. However, colony D12 exhibits a distinctively different pattern and was selected for further analysis. Radar plots allowed us to simultaneously assess the overall activity of a mutant (distance to the center) and the substrate utilization pattern (shape of the plot). The typical patterns found were (a) similar to wt in shape and level of activity, (b) similar to wt in shape with lower levels of activity, (c) different from wt in shape but with very low levels of activity, and (d) different from wt in shape and with significant activity. Radar plots coupled with simple activity bar graphs like the ones shown in Figure 2 were used to identify colonies showing evidence of both changes in the substrate usage pattern and an improvement in the use of Pyr, or more generally, toward aliphatic 2-keto acids as substrates.

Of the 12 positions randomized in the first round, 10 did not contribute colonies with improved activity toward Pyr or other aliphatic 2-keto acids. The remaining two, however, showed significantly higher activity than wt activity toward Pyr for some colonies. For example, when library A460X was assayed, several colonies showed radar plots that significantly departed from the shape of the wt plot, while maintaining considerable overall decarboxylase activity. Sequencing of the plasmid DNA isolated from these colonies showed that Ala460 had been replaced by one of leucine, phenylalanine, or tyrosine. While different to that of the wt enzyme, the radar plots of the A460L, A460F, and A460Y variants were similar, and each still showed evidence of significant decarboxylase activity. This is highlighted in Figures 4A and

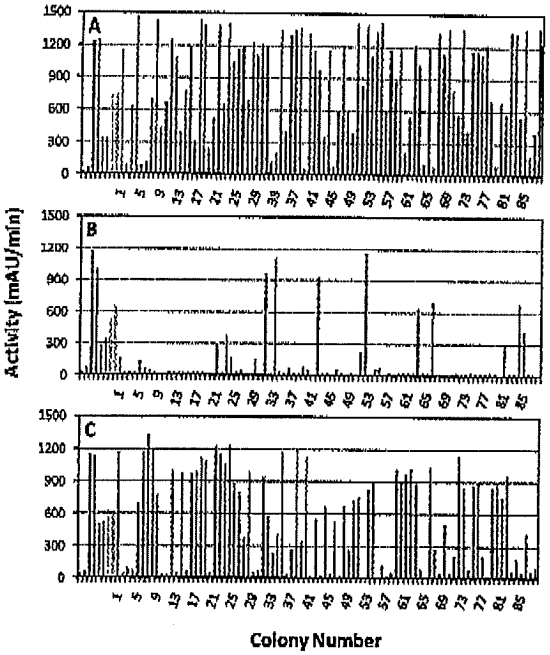

FIGURE 2: Activity plots of 88 colonies obtained from a library of site saturation mutants of (A) Phe464, (B) Gly401, and (C) Ala460 as described in Materials and Methods. The activity of whole cell extracts was measured with 1 mM benzoylformate. In each case, the first 8 bar comprise the following controls: FMJ39(DE3) containing pET24d (black), WT BFDC (blue), BFDC A460I (green), and BFDC F464I (orange).

B, which show radar plots obtained with crude extracts from wt and A460Y colonies, respectively. Overall, this substitution appears to lower the activity of the enzyme toward the natural substrate BF and increase the activity toward the aliphatic substrates.

Conversely, the radar plots obtained from colonies produced with the T377X library were not so readily interpreted. When the bar graphs of the colonies were analyzed, several colonies showed an increase in activity toward Pyr while still maintaining high activity toward BF. Surprisingly, this was accompanied by significantly decreased activity toward larger aliphatic 2-keto acids (2KH, 2KP, and 2KB). Sequencing showed that these colonies contained the BFDC T377L mutation, and a typical radar plot for this variant is provided in Figure 4C.

For a second round of site saturation mutagenesis, A460Y and T377L were employed as the parental plasmids. Again, the primers shown in Table 1 were used, with the exception of G401X and L403X. The initial screening showed that mutations in Gly401 (Figure 2) and Leu403 (data not shown) resulted in enzyme variants with low levels of activity. The reduced activity observed with variants of Leu403 is not surprising as it is the bulky hydrophobic amino acid that helps keep the cofactor in the V conformation necessary for the activity of BFDC and other ThDP-dependent enzymes (*31*). The controls included the parental strain in each case, and although radar plots were analyzed, in this round, the search was primarily focused on variants that afforded improved decarboxylation of Pyr. Fortunately, the activity data acquired in the second round of mutagenesis were more consistent than data obtained in the initial round because the starting activity toward Pyr of the

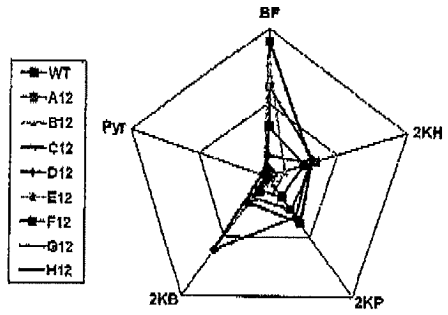

FIGURE 3: Radar plots depicting activity data collected using the screening assay. The axes represent activity of whole cell extracts expressed in mAU/min. The scale is identical for each plot and ranges from 0 to 1000 mAU/min. The activity data from each plate with each of the five substrates analyzed were separated in groups of 8 colonies, and each group was plotted in a separate radar plot together with the wt control from the same plate (black). This allowed for the rapid visual identification of colonies with a different pattern of substrate utilization.

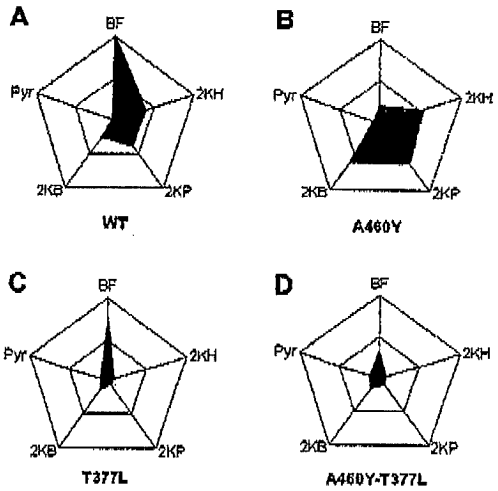

FIGURE 4: Radar plots showing the activity of single colonies in the screening assay. The axes represent the activity of whole cell extracts in mAU/min and are all in the same scale from 0 to 1200 mAU/min. (A) wt BFDC; (B) A460Y; (C) T377L; (D) T377L-A460Y.

parental strains was well above that of the background. As it happened, the only variant that significantly improved Pyr decarboxylation was the double mutant T377L-A460Y, and comfortingly, this variant was identified independently from both parental plasmids. Other mutants were found with changed patterns of substrate utilization as assessed in the radar plots, but none of them had improved activity toward Pyr; therefore, they were not selected for further examination at this time. The radar plot from a colony with the T377L-A460Y mutations is shown in Figure 4D.

Characterization of BFDC Variants. Plasmids carrying the mutations A460Y, T377L, and T377L-A460Y were transformed into BL21(DE3)pLysS cells and 2 L cultures were grown. The mutant enzymes were purified to apparent homogeneity as assessed by SDS−PAGE and their steady-state kinetics characterized using the enzyme assay described under Materials and Methods. The results are summarized in Table 3. The aliphatic

Table 3: Steady-State Kinetic Characterization of BFDC Variants Showing Improved PDC Activity.[a,b]

BFDC variant	parameter	BF	2KH	2KP	2KB	Pyr
wt	k_{cat} (s^{-1})	320 ± 5	5.3 ± 0.3	11 ± 1	4 ± 1	–
	K_m (mM)	0.27 ± 0.02	4.1 ± 0.1	6.0 ± 0.5	7.5 ± 0.6	–
	k_{cat}/K_M (mM^{-1} s^{-1})	1180 (1)	1.3 (1)	1.8 (1)	0.5 (1)	0.012 (1)
A460Y	k_{cat} (s^{-1})	1.7 ± 0.3	4.4 ± 0.2	6.2 ± 0.2	6.0 ± 0.4	1.4 ± 0.2
	K_m (mM)	0.04 ± 0.01	0.28 ± 0.05	0.28 ± 0.03	1.3 ± 0.2	21 ± 1
	k_{cat}/K_m (mM^{-1} s^{-1})	43 (0.036)	16 (12)	22 (12)	4.6 (9)	0.065 (5)
T377L	k_{cat} (s^{-1})	110 ± 5	1.1 ± 0.1	3.3 ± 0.1	7.5 ± 0.3	2.0 ± 0.2
	K_m (mM)	0.45 ± 0.05	1.3 ± 0.3	1.1 ± 0.1	4.3 ± 0.4	4.8 ± 0.2
	k_{cat}/K_m (mM^{-1} s^{-1})	244 (0.2)	0.86 (0.6)	3 (1.6)	1.7 (3)	0.42 (35)
T377L-A460Y	k_{cat} (s^{-1})	25 ± 2	1.2 ± 0.1	0.81 ± 0.05	5.8 ± 0.2	3.6 ± 0.3
	K_m (mM)	1.5 ± 0.2	0.15 ± 0.02	0.10 ± 0.01	0.42 ± 0.02	2.0 ± 0.1
	k_{cat}/K_m (mM^{-1} s^{-1})	16 (0.013)	8 (6)	8.1 (4.5)	14 (28)	1.8 (150)

[a] In parentheses is the -fold increase over wt BFDC for each substrate. [b] Values are mean of 3 independent determinations ± SE.

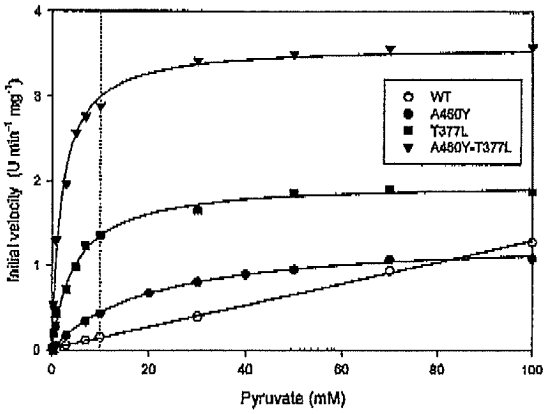

FIGURE 5: Initial velocity as a function of Pyr concentration for BFDC variants. The dotted line marks the Pyr concentration used in the screening assay. Assays were carried out at 30 °C in 100 mM potasium phosphate buffer at pH 6.0.

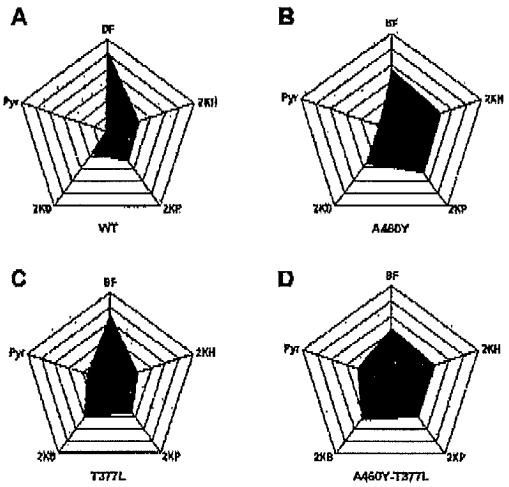

FIGURE 6: Radar plots showing different patterns of substrate utilization for purified BFDC variants. The axes represent k_{cat}/K_M (mM^{-1} s^{-1}) and are all in the same logarithmic scale (0.01 to 10000), with gridlines signaling increments of 1 order of magnitude.

substrates, 2KH, 2KP, and 2KB, are turned over with similar efficiency, albeit ca. 3 orders of magnitude lower than that for BF. As reported previously, wt BFDC was found to decarboxylate Pyr (*12*), but it could not be saturated with this substrate (Figure 5). Consequently, it was necessary to study the activity with Pyr under V/K conditions, and it was found that the k_{cat}/K_m value for Pyr was nearly 5 orders of magnitude lower than that of the BF (Table 3). Although the mutants all show a decrease in their ability to decarboxylate BF, they still show sufficient activity to allow easy kinetic analysis. By some measures, A460Y shows the greatest changes with both the largest (~200-fold) decrease in k_{cat} value and the only observed decrease in K_m value for benzoylformate. The variants all show an increase in binding affinity for aliphatic substrates. The greatest improvement in catalytic efficiency is provided by the double mutant, which shows a 150-fold increase in k_{cat}/K_m for pyruvate. This improvement is clearly illustrated in Figure 5, which shows the dependence of the reaction rate on Pyr concentration. The wt enzyme shows a linear increase in rate for Pyr concentrations as high as 100 mM. By contrast, the three variants identified in this work show Michaelis–Menten kinetics and reach saturation well under 100 mM Pyr.

The radar plots in Figure 6 illustrate the pattern of substrate utilization of purified wt BFDC and mutants. In this case, the axes represent the k_{cat}/K_m value, but unlike the plots in Figures 3 and 4, a logarithmic scale was employed. While it is clear that wt BFDC has its maximum efficiency toward BF, the k_{cat}/K_m values of the mutants appear much more evenly distributed between the different substrates. The almost pentagonal shape of the graph corresponding to variant A460Y-T377 conveys the fact that this mutant uses all substrates with comparable efficiency.

DISCUSSION

Homologous enzymes, often grouped together in superfamilies, generally use the same protein scaffold and a chemical mechanism that employs the same elementary chemical step (*32*). As such, swapping of activities between superfamily members presents a test case for engineering of active sites (*33*). Recent reviews have documented many examples to show that new activities are readily accessible, often through a single mutation (*33*, *34*). Then again, this is not always true, as divergent evolution can bring about the insertion and deletion of residues (*35*) that necessitates a more aggressive approach to mutagenesis (*36*).

Structural (*11*) and evolutionary (*37*) analysis suggest that the ThDP-dependent family of enzymes has evolved from a single